MPMI Vol. 37, No. 3, 2024, pp. 264–276, https://doi.org/10.1094/MPMI-09-23-0136-FI

Mutagenesis of Wheat Powdery Mildew Reveals a Single Gene Controlling Both NLR and Tandem Kinase-Mediated Immunity

Zoe Bernasconi,[1] Ursin Stirnemann,[1] Matthias Heuberger,[1] Alexandros G. Sotiropoulos,[1,2] Johannes Graf,[1] Thomas Wicker,[1] Beat Keller,[1,†] and Javier Sánchez-Martín[1,3,†]

[1] Department of Plant and Microbial Biology, University of Zurich, Zurich, Switzerland
[2] Centre for Crop Health, University of Southern Queensland, Darling Heights, Queensland, Australia
[3] Department of Microbiology and Genetics, Spanish-Portuguese Agricultural Research Centre (CIALE), University of Salamanca, Salamanca, Spain

Accepted for publication 31 October 2023.

***Blumeria graminis* f. sp. *tritici* (*Bgt*) is a globally important fungal wheat pathogen. Some wheat genotypes contain powdery mildew resistance (*Pm*) genes encoding immune receptors that recognize specific fungal-secreted effector proteins, defined as avirulence (Avr) factors. Identifying Avr factors is vital for understanding the mechanisms, functioning, and durability of wheat resistance. Here, we present AvrXpose, an approach to identify *Avr* genes in *Bgt* by generating gain-of-virulence mutants on *Pm* genes. We first identified six *Bgt* mutants with gain of virulence on *Pm3b* and *Pm3c*. They all had point mutations, deletions or insertions of transposable elements within the corresponding *AvrPm3*$^{b2/c2}$ gene or its promoter region. We further selected six mutants on *Pm3a*, aiming to identify the yet unknown AvrPm3^{a3} recognized by Pm3a, in addition to the previously described AvrPm3$^{a2/f2}$. Surprisingly, *Pm3a* virulence in the obtained mutants was always accompanied by an additional gain of virulence on the unrelated tandem kinase resistance gene *WTK4*. No virulence toward 11 additional *R* genes tested was observed, indicating that the gain of virulence was specific for *Pm3a* and *WTK4*. Several independently obtained *Pm3a-WTK4* mutants have mutations in *Bgt-646*, a gene encoding a putative, nonsecreted ankyrin repeat-containing protein. Gene expression analysis suggests that *Bgt-646* regulates a subset of effector genes. We conclude that *Bgt-646* is a common factor required for avirulence on both a specific nucleotide-binding leucine-rich repeat and a WTK immune receptor. Our findings suggest that, beyond effectors, another type of pathogen protein can control the race-specific interaction between powdery mildew and wheat.**

Keywords: avirulence factors, AvrXpose, *Blumeria graminis*, effectors, mutagenesis, NLR, race-specific resistance, tandem kinase proteins, transposable elements, wheat

Plant pathogens secrete effector proteins that interfere with host metabolism and suppress its immune response (Dodds and Rathjen 2010; Lo Presti et al. 2015). Host resistance (*R*) genes encode intracellular receptors that directly or indirectly recognize pathogen effectors. This recognition results in effector-triggered immunity (Jones and Dangl 2006) and frequently culminates in a hypersensitive response and cell death. Recognized effectors are also called avirulence (Avr) effectors and are considered disadvantageous for the pathogen. Consequently, strong host resistance results in an efficient selection for mutated (or deleted) effectors or reduced effector expression to avoid recognition (Lo Presti et al. 2015; Sánchez-Vallet et al. 2018). Thus, there is a trade-off between avoidance of recognition and the loss of effector gene function, which could result in a fitness cost (Sánchez-Vallet et al. 2018).

Powdery mildews form one of the most widespread group of plant pathogens, infecting an estimated 10,000 plant species (Takamatsu 2004). Among them are crop plants, including bread wheat, infected by wheat powdery mildew (*Blumeria graminis* f. sp. *tritici* [*Bgt*]) (Sánchez-Martín et al. 2018). Powdery mildews are obligate biotrophic, highly specialized pathogens that need living host tissue to proliferate. Previous work on the wheat–*Bgt* pathosystem mostly focused on *R* genes encoding nucleotide-binding leucine-rich repeat (NLR) immune receptors. One of the most studied NLR-encoding *R* genes conferring resistance to *Bgt* is the allelic series *Pm3* (Yahiaoui et al. 2006). It has been shown that different Pm3 variants recognize sequence-unrelated effectors of *Bgt*. Pm3a and Pm3f recognize the same Avr, AvrPm3$^{a2/f2}$ (Bourras et al. 2015), while Pm3b and Pm3c recognize AvrPm3$^{b2/c2}$ (Bourras et al. 2019). *Pm3a* and *Pm3b* have an extended resistance spectrum compared with their companion alleles, *Pm3f* and *Pm3c*, respectively (Stirnweis et al. 2014). Brunner et al. (2010) tested a large set of *Bgt* isolates and found that *Pm3a*-mediated resistance against 454 isolates,

†Corresponding authors: B. Keller; bkeller@botinst.uzh.ch, and J. Sánchez-Martín; j.sanchezmartin@usal.es

Author contributions: Z.B., J.S.-M., and B.K. conceived the experiments, interpreted results, and wrote the manuscript. Z.B. and U.S. produced the *Bgt* mutants and performed the phenotyping experiments. U.S. performed the RT-qPCR experiments. Z.B., T.W., A.G.S., J.G., and M.H. contributed to the bioinformatic analyses. All authors have read and agreed to the published version of the article.

Funding: This work was supported by the Schweizerischer Nationalfonds zur Förderung der Wissenschaftlichen Forschung grants 310030B_182833 and 310030_204165. J. Sánchez-Martín is the recipient of the grant "Ramon y Cajal" Fellowship RYC2021-032699-I funded by Ministerio de Ciencia e Innovación/Agencia Estatal de Investigación.

e-Xtra: Supplementary material is available online.

The author(s) declare no conflict of interest.

including all 173 isolates avirulent on *Pm3f*, thus exhibiting an extended resistance spectrum compared with *Pm3f*. Similarly, the *Pm3b* allele showed broader resistance than the narrow-spectrum *Pm3c* allele. Genetic analysis in mapping populations suggested the existence of additional pathogen components involved in different Pm3-AvrPm3 interactions, which may explain the differences in the resistance spectra of the *Pm3* alleles (Bourras et al. 2015, 2016). The *Pm3-AvrPm3* interaction is further complicated by the presence of a suppressor gene of avirulence in some mildew isolates (*SvrPm3*; Bourras et al. 2015; Parlange et al. 2015), which was proposed to encode a general factor involved in all Pm3-AvrPm3 interactions by masking the presence of AvrPm3 effectors, thus blocking a resistance response. In addition, $AvrPm3^{a2/f2}$ is present in multiple copies in different *Bgt* isolates (Müller et al. 2019). *Pm3-AvrPm3* is not a unique case of a noncanonical gene-for-gene interaction: It has been reported for other *R* genes, such as *Pm1a* (Hewitt et al. 2021; Kloppe et al. 2023), that multiple pathogen components determine the interaction with the host.

In recent years, novel types of immune receptors have been described as conferring race-specific resistance in wheat (Sánchez-Martín and Keller 2021). These include, in the case of wheat powdery mildew, tandem kinase proteins, such as *Pm24* (Lu et al. 2020) and *WTK4* (Gaurav et al. 2022), and other kinase-fusion proteins, such as *Pm4* (Sánchez-Martín et al. 2021). However, little is known about how these novel proteins function at the molecular level. Rpg1, identified by Brueggeman et al. (2002), is the most-studied tandem kinase protein. It confers race-specific resistance to stem rust in barley and was observed to be phosphorylated and degraded upon infection with avirulent rust spores. Two rust proteins, a fibronectin type III and breast cancer type 1 susceptibility protein and a vacuolar protein, were described as determinants of Rpg1 phosphorylation and hypersensitive response in resistant cultivars (Nirmala et al. 2011). However, there is limited knowledge about the recognition mechanisms of other tandem kinase or kinase-fusion proteins and the specific pathogen components with which they interact (Klymiuk et al. 2021). The identification of the Avr components recognized by unconventional R proteins is essential for understanding the activation of the plant immune system by these novel immune receptors.

All *Bgt* Avr effectors identified to date are small (fewer than 159 amino acids) and have a signal peptide and conserved cysteine residues at defined positions, and all share a predicted or confirmed RNAse-like 3D structure (Bourras et al. 2016, 2019; Cao et al. 2023; McNally et al. 2018; Praz et al. 2017). Genomic and transcriptomic genome-wide association studies (GWAS), quantitative trait locus mapping, and effector benchmarking have been used to identify *Avr* genes in cereal powdery mildews (Bourras et al. 2015, 2019; Hewitt et al. 2021; Lu et al. 2016; Praz et al. 2017; Saur et al. 2019). However, these methods have some limitations, such as the need to maintain and sequence large populations, the bias bestowed by the reference genome(s), and the requirement for genetic variability and recombination at the *Avr* loci. The lack of stable transformation protocols for *Bgt* further hampers *Avr* identification and characterization. In other classes of obligate fungal pathogens, some attempts have been made to obtain mutants with gain of virulence: for example, through ethyl-methane sulfonate (EMS) treatment in wheat rusts (Kangara et al. 2020; Li et al. 2019) and barley powdery mildew (Sherwood et al. 1991). EMS mutagenesis allowed the identification of *AvrSr35* in stem rust (Salcedo et al. 2017), while spontaneous mutants contributed to the identification of *AvrSr50* (Chen et al. 2017) and *AvrSr27* (Upadhyaya et al. 2021). Recently, ultraviolet light (UV) mutagenesis has been used in quasi-evolutionary experiments to study induced mutations involved in fungal viability and pathogenesis in barley powdery mildew (Barsoum et al. 2020), but mutagenesis has not been used to identify *Avr* factors in cereal powdery mildews.

In this work, we aimed to establish a methodology to identify *Avr* factors using UV mutagenesis to circumvent some limitations of the other *Avr* identification approaches. As a proof of concept, we first demonstrate the efficiency of our approach by identifying six and two mutants of the $AvrPm3^{b2/c2}$ and $AvrPm3^{a2/f2}$ avirulence genes, respectively, revealing different molecular mechanisms of escape from recognition. Further, because mutants virulent on *Pm3f* did not gain virulence on *Pm3a*, we used a *Pm3f*-virulent mutant as a background to apply AvrXpose to the case of *Pm3a*, identifying six *Pm3a* virulent mutants. Finally, we show that our approach can identify a pathogen factor controlling avirulence on two different types of *R* genes, an *NLR* and a *WTK*. We conclude that classical Avr effectors are only one type of pathogen factor contributing to the specificity of R-Avr interactions.

Results

Gain-of-virulence *Bgt* mutants on *Pm3b* and *Pm3c* generated by UV mutagenesis reveal different mechanisms of escape from recognition

We wanted to establish a pipeline based on UV irradiation to induce mutations in genes controlling avirulence on different alleles of the *Pm3* gene. We developed an approach that we named "AvrXpose." In three rounds, we mutagenized and propagated the *Bgt* isolate CHE_96224, avirulent on all tested *Pm3* alleles, on the powdery mildew-susceptible line Kanzler. Mutagenized spore mixtures were then used to infect near-isogenic lines (NILs) containing one of the *R* genes *Pm3a*, *Pm3b*, *Pm3c*, *Pm3d*, *Pm3f* or a transgenic line containing *Pm3e* (E#2) to select *Pm3* allele gain-of-virulence mutants (Fig. 1).

Because virulence to *Pm3c* was suggested to be determined by only one avirulence component ($AvrPm3^{b2/c2}$; Bourras et al. 2015, 2019), we assumed that a gain of virulence on *Pm3c* would result from a single mutation in the known *Avr*. Hence, we first tested the feasibility of our method by identifying $AvrPm3^{b2/c2}$ mutants. In addition, we also wanted to determine whether it was feasible to obtain mutants virulent on *Pm3b*, as it shows broader resistance than *Pm3c* (Brunner et al. 2010; Stirnweis et al. 2014). We obtained six independent *Bgt* mutants with simultaneous gain of virulence on both *Pm3b* and *Pm3c* (hereafter, 3BC mutants) by selecting them on wheat lines containing either *Pm3b* or *Pm3c* (Fig. 2A). Notably, the 3BC mutants remained avirulent on the other *Pm3* alleles tested (*Pm3a*, *Pm3d*, *Pm3e*, and *Pm3f*; Supplementary Fig. S1). To further investigate the specificity of the gain of virulence on other *Pm* resistance genes, we also infected NILs containing *Pm1a*, *Pm2*, *Pm4a*, *Pm4b*, *Pm8*, *Pm24*, and three *Aegilops tauschii* lines containing *WTK4* with the mutants. We confirmed that the 3BC mutants were still avirulent on them as well, with the exception of *Pm1a* and *Pm8*, for which the parental isolate CHE_96224 is virulent (Supplementary Fig. S1). This demonstrates that the mutants are affected specifically in avirulence to *Pm3b* and *Pm3c*.

Next, we wanted to determine the genetic cause of the gain of virulence. Illumina whole-genome sequencing followed by single-nucleotide polymorphism (SNP) calling to the wild-type, non-mutated *Bgt* isolate CHE_96224 revealed between 253 and 975 SNPs and small (<7 bp) insertions/deletions (indels) per *Bgt* isolate (Table 1). Among these SNPs, 41 to 503 were unique mutations, that is, present only in one mutant of the same mutant group (Table 1; Supplementary Tables S1 to S3). We observed that the discrepancy between total and unique SNPs was mostly caused by SNP calling artifacts. In transposable element (TE)-rich, repetitive, or low sequencing depth regions, there was a certain level of heterozygosity and ambiguous mapping in the

reads of all *Bgt* mutants, which led to some wrong SNP calling. Nonetheless, we eliminated most of these cases by filtering for unique mutations. This issue was previously encountered by Barsoum et al. (2020), who also filtered mutations by uniqueness and visually inspected all variants individually to exclude false positives.

Additionally, we searched for gene deletions by examining the average depth of sequencing coverage as well as TE insertions using the TE detection software Detettore (Stritt and Roulin 2021). We then compared all the variants from the six mutants with one another and examined the mutation overlap.

All 3BC mutants had a mutant variant in (or near) the known *AvrPm3*$^{b2/c2}$ gene (Fig. 2A; Supplementary Table S4). Mutant 3BC_1 had a 1-bp deletion in the gene's coding sequence, causing a frameshift and a premature STOP codon at amino acid position 67. Sequence coverage analysis showed that mutant 3BC_2 had a 9.5-kb chromosomal deletion where the *AvrPm3*$^{b2/c2}$ gene is embedded (Supplementary Table S4). Detettore revealed that mutants 3BC_3 and 3BC_4 both had insertions of *RII_Itera* family non-long terminal repeat (non-LTR) retrotransposons between 467 and 470 bp upstream of the ATG start codon of *AvrPm3*$^{b2/c2}$ (Fig. 2A; Table 2). By de novo assembling the *AvrPm3*$^{b2/c2}$ locus in both mutants, we confirmed that they had independent TE insertions, because mutant 3BC_4 had an 80-bp DNA fragment from chromosome 1 inserted into the region in addition to the *RII_Itera* element. In contrast, in mutant 3BC_3, only the *RII_Itera* element was inserted (Supplementary Fig. S2, Supplementary Extended Data). The *RII_Itera* family of retrotransposons is present in high copy number in the genome of CHE_96224 (107 intact copies with a length of more than 5,000 bp; Table 2). We de novo assembled the *AvrPm3*$^{b2/c2}$ region for mutant 3BC_5 and confirmed that the gene coding sequence was disrupted by a *Gypsy* LTR retrotransposon insertion (Fig. 2A; Table 2; Supplementary Fig. S2). Part of the TE sequence present in the de novo assembly allowed us to assign the TE insertion to a novel TE family (newly named *RLG_Stef*). In contrast to *RII_Itera*, *RLG_Stef* retrotransposons are present in low copy number in CHE_96224 (17 copies with a length of more than 5,000 bp; Table 2).

For mutant 3BC_6, visual inspection of the genomic mapping file with the integrative genomics viewer IGV revealed an irregularity in the sequence of the *AvrPm3*$^{b2/c2}$ promoter region, 1,186 bp before the start of the gene, where a gap in sequence coverage was flanked by reads whose mate reads mapped to a different chromosome, indicating an insertion in this region. Although the Detettore software did not indicate a TE insertion there, this pattern was highly similar to the TE insertions of the three 3BC insertion mutants. Thus, we de novo assembled the

Table 1. Number and types of sequence variants present in the 3BC, 3F, and 3F+A *Blumeria graminis* f. sp. *tritici* (*Bgt*) mutants

Parental isolate	Mutant group	Mutant name	SNPs: whole genome[a]	Unique SNPs[b]	GPV: total[c]	GPV: SNPs	GPV: copy number variations	GPV: TE insertions
CHE_96224	3BC	3BC_1	582	125	23	22	–	1
		3BC_2	253	84	7	5	1	1
		3BC_3	572	125	5	4	–	1
		3BC_4	321	62	9	3	–	6
		3BC_5	267	67	3	2	–	1
		3BC_6	381	58	6	2	–	4
	3F	3F_1	973	508	13	7	5	1
		3F_2	640	234	26	26	–	–
3F_1	3F+A	3F+A_1	831	89	8	8	–	–
		3F+A_2	754	116	24	20	–	4
		3F+A_3	899	90	8	8	–	–
		3F+A_4	975	98	14	13	–	1
		3F+A_5	822	78	10	6	–	4
		3F+A_6	822	41	4	2	–	2

[a] Total number of single-nucleotide polymorphisms (SNPs) compared with the parental isolate (CHE_96224 or 3F_1) detected by Freebayes and filtered with quality criteria as described in "Materials and Methods." Also included in this category are small insertions or deletions (max. 7 bp), that can be detected with Freebayes. Bigger deletions are listed in the category "GPV: copy number variations."
[b] Number of unique SNPs, e.g., SNPs only present in one isolate and not in any other isolate of the same mutant group (Supplementary Tables S1 to S3).
[c] Gene-proximal variants (GPV) include unique SNPs or deletions closer than 1.5 kb to genes, and transposable element (TE) insertions closer than 2 kb. All variants have been visually inspected and confirmed with IGV and/or validated via PCR. The different categories of GPV are listed in the following rows. The description of the affected genes can be found in Supplementary Table S4.

Table 2. Transposable element (TE) insertions in proximity of *AvrPm3*$^{b2/c2}$ in the 3BC mutants

Mutant	TE class[a]	TE name	TE distance to *AvrPm3*$^{b2/c2}$	TE description[b]
3BC_3	Non-LTR retrotransposon (LINE), *RII*	*RII_Itera*	470 bp	Consensus length: 5,392 bp; number of full copies present in CHE_96224: 107 (high copy TE)
3BC_4	Non-LTR retrotransposon (LINE), *RII*	*RII_Itera*	467 bp	Consensus length: 5,392 bp; number of full copies present in CHE_96224: 107 (high copy TE). 80 bp from chromosome 1 inserted additionally to the *RII_Itera* element.
3BC_5	LTR retrotransposon, *Gypsy*	*RLG_Stef*	0 bp (insertion in the CDS)	Consensus length: 5,723 bp; number of full copies present in CHE_96224: 17 (low copy TE)
3BC_6	LTR retrotransposon, *Copia*	*RLC_Lily*	1,186 bp	Not detected by Detettore, only visual analysis. Length: 5,264 bp; number of full copies present in CHE_96224: 18 (low copy TE)

[a] LTR, long terminal repeat.
[b] The consensus length indicates the length in base pairs (bp) of the consensus sequence of the TE, retrievable from https://www.botinst.uzh.ch/en/research/genetics/thomasWicker/trep-db.html. A TE was considered to be a full copy when the BLAST hit was longer than 5,000 bp.

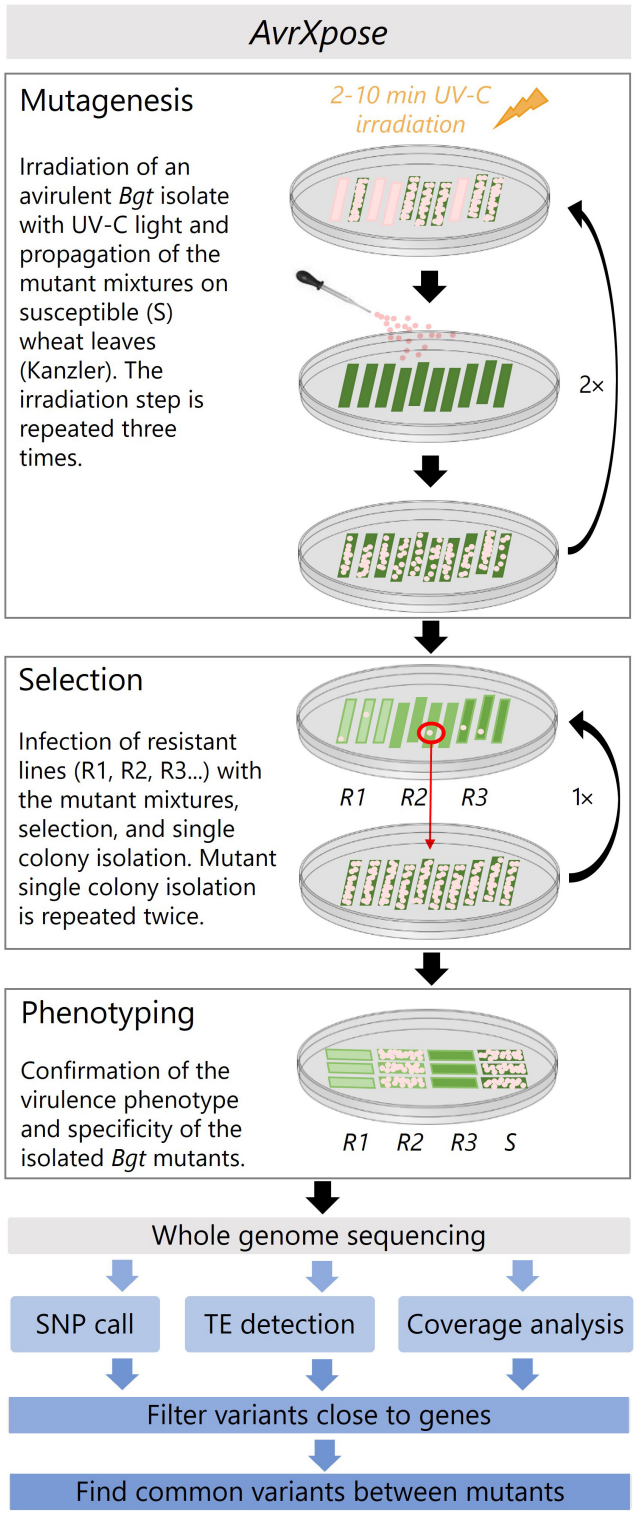

Fig. 1. AvrXpose pipeline to isolate gain-of-virulence *Blumeria graminis* f. sp. *tritici* (*Bgt*) mutants and to unravel the corresponding mutated genes. The first step of AvrXpose includes the identification of *Bgt* mutants with gain of virulence on a specific *R* gene. This is followed by bioinformatic analyses, such as variant calling, transposable element (TE) insertion detection, and coverage analysis, and a final visual confirmation using a genome viewer software (e.g., IGV). Variants that potentially affect genes are selected. Finally, all the variants of *Bgt* mutants with the same gain of virulence are compared, and variants affecting the same genes are selected. These can be further studied and considered as putative avirulence components. NIL, near-isogenic line; SNP, single-nucleotide polymorphism.

AvrPm3$^{b2/c2}$ region for mutant 3BC_6 and detected an insertion of a TE belonging to a previously uncharacterized family of *Copia* LTR retrotransposons (newly named *RLC_Lily*) (Supplementary Fig. S2). We observed that *RLC_Lily* retrotransposons are also present in low copy number in CHE_96224 (18 copies; Table 2).

We performed amplification experiments with long extension times to verify the putative TE insertions. We designed primers to amplify the putative insertions in mutants 3BC_3 and 3BC_4 (Mix_3BC3/4), 3BC_5 (Mix_3BC5), and 3BC_6 (Mix_3BC6). As a control, part of the *AvrPm3*$^{b2/c2}$ gene was amplified (Mix_Avr; Fig. 2B). As expected, no amplification in the large deletion mutant 3BC_2 occurred with any of the primer mixes, and fragments of the expected size were only amplified for CHE_96224 and the point mutation mutant 3BC_1. For the other 3BC mutants, the amplicon size was larger than expected in all putative TE insertion sites, confirming the insertion of foreign DNA in the range of more than 5,000 bp (Fig. 2B), which is consistent with the average size of a full-length TE of the detected TE families (Table 2). No amplification was observed with Mix_3BC6 in mutant 3BC_6, suggesting that insertion size may be larger than in the other mutants. Alternatively, the PCR conditions used were unsuitable for proper amplification of this newly identified TE. We further analyzed the impact of the TE insertions on gene expression. We observed a significant reduction in *AvrPm3*$^{b2/c2}$ expression levels in all 3BC mutants: more than 3-fold in 3BC_1 to up to 90-fold in 3BC_4 (Fig. 2C). We concluded that modifications of *AvrPm3*$^{b2/c2}$ of different types, that is, point mutations, deletions, or TE insertions causing reduced gene expression and gene disruption, can all lead to loss of recognition by both *Pm3b* and *Pm3c*.

Gain of virulence on *Pm3f* does not cause virulence on the companion *R* gene *Pm3a*

We then set out to identify *Bgt* mutants with gain of virulence on *Pm3f* and *Pm3a*. We found two *Bgt* mutants with gain of virulence on *Pm3f* (hereafter referred to as 3F mutants), and both remained avirulent on *Pm3a* (Supplementary Fig. S3), although the two *R* genes have an overlapping resistance spectrum. This finding supported the hypothesis that in addition to the commonly recognized AvrPm3$^{a2/f2}$, a second Avr is recognized by Pm3a, but not by Pm3f (Bourras et al. 2015). Mutant 3F_1 had a 107-kb deletion in the *AvrPm3*$^{a2/f2}$ locus, resulting in the loss of the two *AvrPm3*$^{a2/f2}$ copies and four additional genes (Supplementary Table S4), thus explaining the gain of virulence on *Pm3f*. Interestingly, mutant 3F_2 had a single SNP in the coding region of *AvrPm3*$^{a2/f2}$ in about 50% of the reads (F95Y). Visual inspection of the genomic mapping file of mutant 3F_2 was necessary to discover this point mutation, as the filtering criteria used for the SNP call were too stringent, requiring the variant to be present in at least 70% of the reads to be considered a SNP. Previous studies have shown that CHE_96224 has two copies of *AvrPm3*$^{a2/f2}$ based on examination of sequencing coverage (Müller et al. 2019). However, distinguishing the two copies at the genome level is not possible with the available assembly. We therefore hypothesized that in mutant 3F_2, one of the *AvrPm3*$^{a2/f2}$ copies is intact, while the other is mutated. McNally et al. (2018) found natural *Bgt* isolates with a single point mutation at the same position (F95L) and defined it as a virulent allele, as all isolates with this mutation were virulent on *Pm3f*. Although the natural mutation is different from the one present in mutant 3F_2, our data support the hypothesis that a single SNP in position 95 confers virulence, implying that this position is critical for the recognition of *AvrPm3*$^{a2/f2}$ by *Pm3f*. Furthermore, the fact that in mutant 3F_2, one copy of *AvrPm3*$^{a2/f2}$ is still intact, while the other has a point

mutation, indicates that one mutated gene copy is sufficient to disrupt recognition. As the two mutants on *Pm3f* were still avirulent on *Pm3a*, we concluded that loss or mutation of *AvrPm3*$^{a2/f2}$ results in disrupted recognition by *Pm3f*, but it is not sufficient to avoid recognition by the broader resistance allele *Pm3a*.

The *Pm3a* gain-of-virulence mutants show additional virulence on a tandem kinase *R* gene

The fact that gain of virulence on *Pm3f* does not lead to virulence on *Pm3a* suggests that Pm3f specifically recognizes AvrPm3$^{a2/f2}$, whereas Pm3a can recognize AvrPm3$^{a2/f2}$, as well as an additional Avr component, hereafter defined as AvrPm3^{a3}, for consistency with previous nomenclature (Bourras et al. 2015). To identify *AvrPm3*^{a3}, we used the large deletion mutant 3F_1 as a parental isolate for a secondary UV mutagenesis to ultimately obtain mutants with gain of virulence on both *Pm3f* and *Pm3a* (3F+A mutants). We identified six 3F+A mutants that were fully virulent on *Pm3a* and *Pm3f*. We wanted to investigate whether the gain of virulence of the 3F+A mutants on *Pm3a* was specific or whether avirulence on other *Pm* genes was also compromised. Accordingly, we performed phenotyping on different wheat NILs containing the resistance genes *Pm1a*, *Pm2*, *Pm3b*, *Pm3c*, *Pm3d*, *Pm3e*, *Pm4a*, *Pm4b*, *Pm8*, and *Pm24*; the wheat 1AL.1RS translocation line Amigo, containing *Pm17*; and four *A. tauschii* lines containing *WTK4*. All six 3F+A mutants remained avirulent on the *Pm* genes encoding NLRs, indicating that NLR-based immunity and recognition were specifically compromised only for *Pm3a* (Fig. 3; Supplementary Fig. S4). Avirulence to the kinase-fusion proteins Pm4a and Pm4b and to the tandem kinase protein Pm24 was also not affected. Surprisingly, all six 3F+A mutants, besides being virulent on *Pm3f* and *Pm3a*, showed a gain of virulence on the *A. tauschii* accessions carrying the tandem kinase resistance gene *WTK4* (Fig. 3; Supplementary Fig. S4). These data suggest that there is a common pathway specifically controlling avirulence on the NLR *Pm3a* and the tandem kinase immune receptor *WTK4*.

Sequencing of *Pm3a* virulent mutants reveals mutations in *Bgt-646*, an ankyrin repeat-containing gene conserved across different powdery mildew species

We then wanted to determine the genetic cause of the gain of virulence on *Pm3a* and *WTK4*. Whole-genome sequencing and mutation-overlap analysis revealed that three independent 3F+A mutants, 3F+A_1, 3F+A_2, and 3F+A_3, had mutations in the

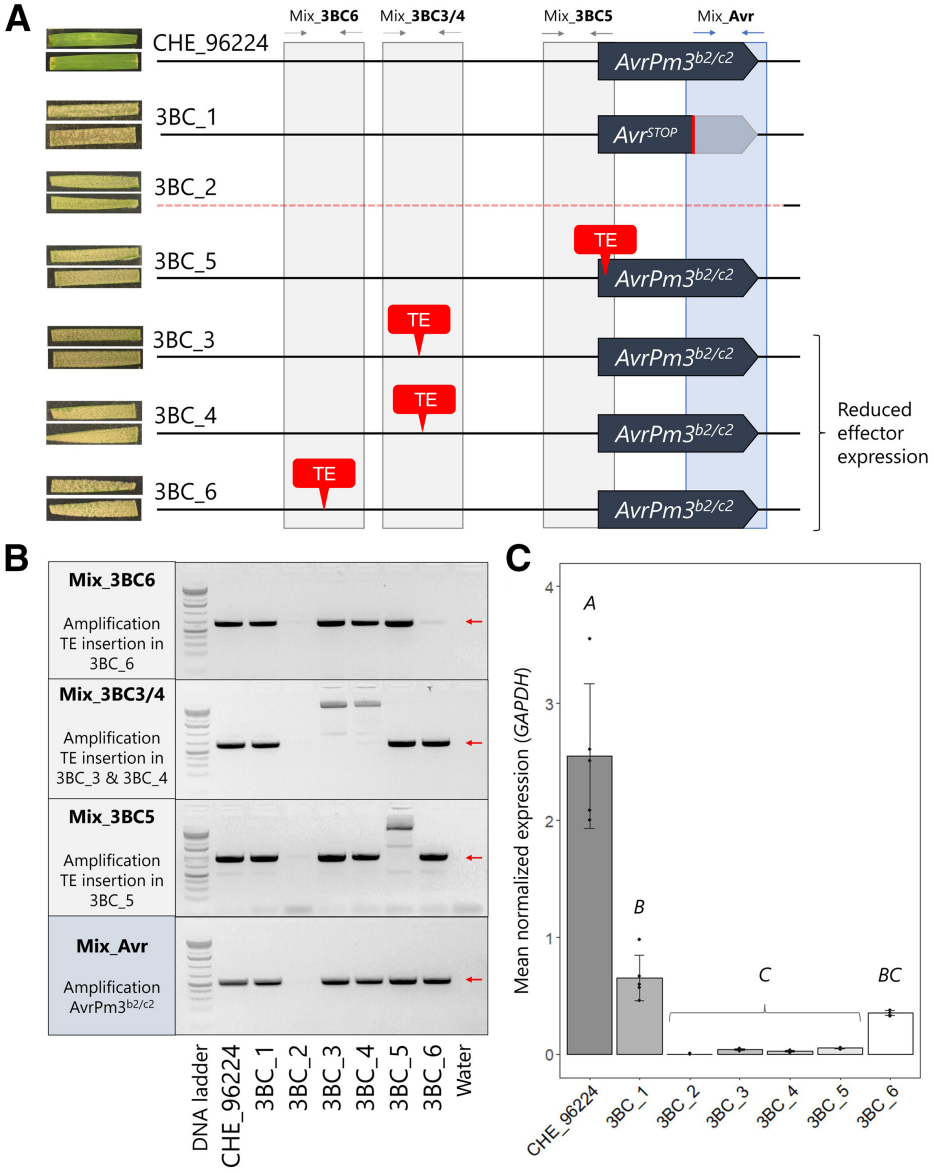

Fig. 2. The 3BC mutants reveal multiple mechanisms of loss-of-function modifications of *AvrPm3*$^{b2/c2}$. **A,** Leaves of Chul/8*Chancellor (*Pm3b*; upper leaf) and Sonora/8*Chancellor (*Pm3c*; lower leaf) infected with the corresponding isolate. Transposable element (TE) insertions are represented with red boxes. The gray and blue boxes indicate the fragments amplified with the different primer mixes. The representation is not to scale. **B,** PCR amplification of the *AvrPm3*$^{b2/c2}$ promoter regions where some mutants have either a deletion or a TE insertion. The expected fragment length of CHE_96224 is indicated with a red arrow. **C,** The expression of *AvrPm3*$^{b2/c2}$ is reduced in all 3BC mutants at 2 days postinfection. The expression normalized to the reference gene *GAPDH* is depicted on the *y* axis. Significance groups were calculated with analysis of variance (ANOVA) followed by a Tukey's HSD test (Supplementary Table S11); bars with the same letter are not significantly different.

Bgt-646 gene (Fig. 4). In addition, 3F+A_4 had an SNP 2.7 kb upstream of *Bgt-646* that did not affect its expression, however (Supplementary Fig. S5), and it is therefore unclear whether this mutation is causative for virulence on *Pm3a.* Mutants 3F+A_4, 3F+A_5, and 3F+A_6 did not have other commonly mutated genes (Supplementary Table S4). None of the 3F+A mutants had reduced *Bgt-646* expression compared with the parental isolate 3F_1 (Supplementary Fig. S5). Because at least three of the 3F+A mutants have *Bgt-646* mutated, and no other common mutation was found, we conclude that this gene plays a role in avirulence to *Pm3a*, and also *WTK4*.

Bgt-646 encodes a nuclear protein with a length of 939 amino acids, containing two ankyrin repeat domains of 42 and 92 amino acids (Fig. 4; Supplementary Fig. S6). Because no signal peptide is predicted and the protein is relatively large, *Bgt-646* differs considerably from previously described *Bgt* avirulence components, which are mostly small, secreted effector proteins (Bourras et al. 2015, 2016, 2019; McNally et al. 2018; Praz et al. 2017). We examined the allelic diversity of *Bgt-646* using 102 representative isolates from a global collection of 172 wheat powdery mildew isolates (Sotiropoulos et al. 2022) and found that the gene is highly conserved, with only one isolate having a nonsynonymous SNP at position 376 (K376M). We also included 14 isolates collected on the host plants *Triticum dicoccum* or *Triticum turgidum* subsp. *durum* and found among them eight isolates with a nonsynonymous SNP at position 4 (P4S) and one SNP in the intron (Supplementary Table S5). A single homolog of *Bgt-646* was found in *Blumeria graminis* f. sp. *triticale*, whereas two homologs were identified in *Blumeria graminis* f. sp. *hordei* (100, 97, and 97% protein sequence identity, respectively; Fig. 5; Supplementary Fig. S7). In addition to the homologs in cereal powdery mildews, we identified eight proteins with >70% amino acid sequence identity to Bgt-646, all from different powdery mildew species: four from *Golovinomyces* spp., three from *Erysiphe* spp., and one from *Podosphaera aphanis*, none of which have been studied for functionality (Fig. 5; Supplementary Fig. S7). To better predict a possible function of *Bgt-646*, we searched for homologs in yeast. The closest homolog in yeast is *HOS4*, which is involved in histone deacetylation. However, HOS4 shares 30% protein sequence identity with Bgt-646 only in a short region from amino acid 793 to 889, corresponding to the second ankyrin repeat domain (Fig. 4), while the rest of the protein has very low homology. Additionally, we used structural predictions to find structural homologs of Bgt-646. The closest structural homolog of Bgt-646 predicted with high confidence by the Phyre2 software (Kelley et al. 2015) is ANK2_HUMAN, a human ankyrin repeat protein involved in endocytosis and intracellular protein transport. However, a list

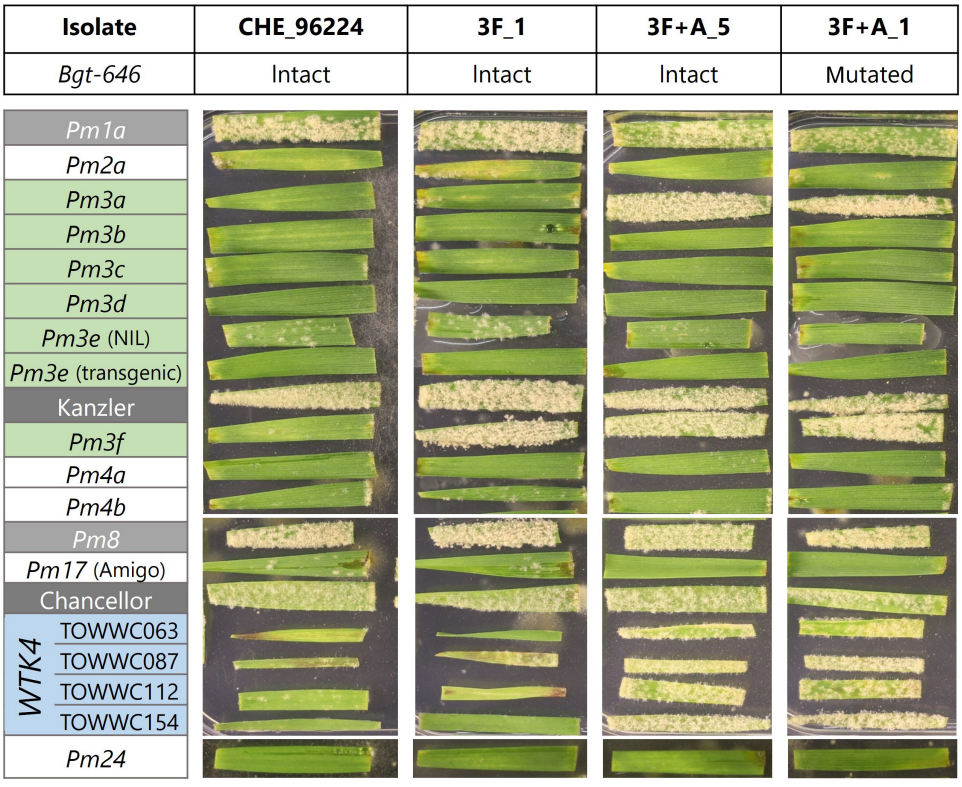

Fig. 3. The 3F+A mutants are virulent on *Pm3a* and *WTK4*, irrespective of *Bgt-646* intactness. Two representatives of the 3F+A mutants, one having *Bgt-646* mutated and the other not, are shown. All other identified 3F+A mutants have comparable phenotypes (Supplementary Fig. S4). Where only the *R* gene is indicated, the corresponding near-isogenic line (NIL) was used. Cultivars and lines susceptible to CHE_96224 (Kanzler, Chancellor, the *Pm1a* NIL, and the *Pm8* NIL) are highlighted in gray. The NILs containing *Pm3* alleles are labeled in green, and the four *WTK4* containing *Aegilops tauschii* lines in blue. The remaining *Pm* lines are in white.

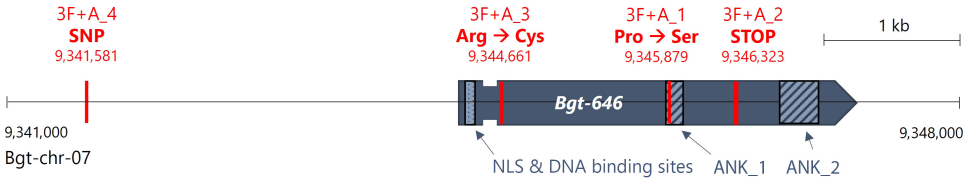

Fig. 4. Schematic representation of the mutations within the Bgt-646 protein or its regulatory region in four 3F+A mutants. The ankyrin repeat domains (ANK_1 and ANK_2) are represented by two gray rectangles with diagonal lines, and the nuclear localization signal (NLS) domain is represented by a gray rectangle with black dots. The mutations in the 3F+A mutants are indicated with red lines.

of more than 100 structural homologs with very high structural homology was generated by Phyre2, possibly because ankyrin repeat proteins are ubiquitous and have highly conserved structures even across different kingdoms despite having multiple functions (Vo et al. 2015). We concluded that these structural predictions may not be informative for Bgt-646 function.

We used additional bioinformatic analyses to gain more insight into the protein domain structure of Bgt-646. DNABIND predicted that Bgt-646 is a DNA-binding protein (Supplementary Table S6). Further analysis with DP-bind and DRNApred also revealed several putative DNA binding sites at the N-terminus, mostly between amino acid residues 33 and 47 (Supplementary Table S7). Most of the predicted DNA binding sites overlap with a nuclear localization signal (NLS), predicted (with low confidence) by PROSITE and (with high confidence) by WoLF PSORT and LOCALIZER (Fig. 4; Supplementary Tables S8 to S10).

We concluded that Bgt-646 is a conserved protein in powdery mildews, whose function cannot be inferred based on functionally characterized homologous proteins. Still, predictions suggest that it has a nuclear localization and can bind DNA.

The gain of virulence on *Pm3a* and *WTK4* is correlated with downregulation of specific effector genes

Given that Bgt-646 does not have a predicted signal peptide, it is most likely not exported from the fungus for uptake by plant cells. Moreover, the gain-of-virulence mutants have lost avirulence on the two unrelated *R* genes, *Pm3a* and *WTK4*. These observations suggest that Bgt-646 has a regulatory function in the fungal pathogen rather than interacting (directly or indirectly) with either Pm3a or WTK4 proteins. Thus, based on its predicted nuclear localization and DNA binding sites (Supplementary Tables S6 to S10), we hypothesized that *Bgt-646* might control avirulence by up- or downregulating the expression of effector genes (e.g., the yet unidentified $AvrPm3^{a3}$ and *AvrWTK4*). Accordingly, we tested the expression of five *Bgt* effectors belonging to different effector families (Müller et al. 2019): *AvrPm2*, $AvrPm3^{a2/f2}$, *SvrPm3*, $AvrPm3^{b2/c2}$, and *Bgt-55150* (the last two being from the same effector family). Because $AvrPm3^{a2/f2}$ is absent in all 3F_1-derived mutants, none of the mutants showed $AvrPm3^{a2/f2}$ expression (Fig. 6). A reduction in *SvrPm3* expression was observed in all 3F+A mutants tested, ranging from 25 to 50% of the expression level in the parental isolate 3F_1 (Fig. 6). Similarly, *Bgt-55150* expression was reduced to 3 to 20% of the expression level in 3F_1 for all 3F+A mutants tested. In contrast, *AvrPm2* and $AvrPm3^{b2/c2}$ expression did not significantly differ from 3F_1 in all 3F+A mutants (Fig. 6).

Thus, the downregulation of effectors appears to be specific, affecting only certain effectors. Even effectors belonging to the same effector family and with high sequence similarity (i.e., $AvrPm3^{b2/c2}$ and *Bgt-55150*; Bourras et al. 2019) have different expression patterns in the 3F+A mutants. We can therefore infer that *Bgt-646*, along with the unknown component(s) mutated in the other 3F+A mutants, potentially affects *Bgt* avirulence by controlling the expression of putative *Avr* genes.

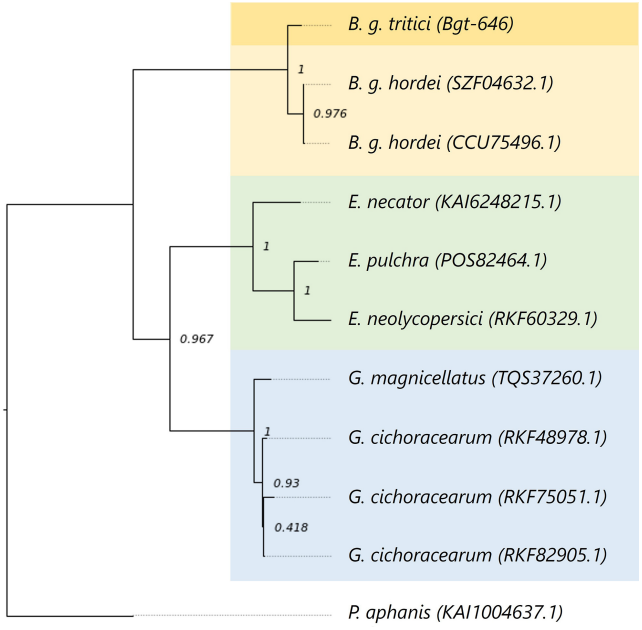

Fig. 5. *Bgt-646* has homologs with more than 70% sequence identity in different powdery mildew species. Only BLAST hits with greater than 97% sequence coverage were considered for constructing the phylogenetic tree. *Bgt-646* is highlighted in dark yellow. The *Podosphaera aphanis* homolog was used as an outgroup.

Discussion

AvrXpose: A novel tool to identify avirulence determinants in powdery mildew

Avr genes in cereal powdery mildews have been cloned through map-based cloning or GWAS or by testing a large number of candidate genes in screening approaches (Bourras et al. 2016, 2019). These methods require the sequencing and maintenance of large pathogen populations, which is time-consuming, costly, and arduous for obligate biotrophic pathogens such as *Bgt*. Besides, these methods rely on natural genetic diversity, which restricts the identification of conserved factors. Moreover, because these methods are based on correlation rather than causation, they can be biased, especially when the molecular interactions are more complex than a gene-for-gene interaction. AvrXpose overcomes some of these limitations. This method only necessitates sequencing and maintaining the reference isolate and the derived mutants, and because it is based on causative mutations, it is less biased. Barsoum et al. (2020) already described the potential of UV mutagenesis to induce phenotype-causing mutations in barley powdery mildew. By adding a selection step after mutagenesis (Fig. 1), we expand the method and make it suitable for forward genetics and functional studies.

By identifying 3BC mutants with a gain of virulence on *Pm3b* and *Pm3c*, we confirmed the suitability of AvrXpose for finding *Avr* genes. AvrXpose also allowed us to discover that variants causing gain of virulence are not only caused by SNPs or indels, but also by larger deletions or TE insertions, which can only be uncovered using different and complementary approaches (coverage analysis or TE detection by Detettore; Stritt and Roulin 2021). For instance, we found that TEs play a role in mildews' escape from recognition, as they were the cause of the gain of virulence in the majority of the 3BC mutants (four out of six). This might be caused by the mechanism of $AvrPm3^{b2/c2}$ recognition, which appears to be easily and completely blocked by changes in the *Avr* expression level. For many years, TE activity has been known to be a key player in pathogen evolution, particularly in powdery mildews (Faino et al. 2016; Frantzeskakis et al. 2018; Wicker et al. 2013). This was also observed in other pathosystems, for example, in wheat blast, for which Inoue et al. (2017) described that the insertion of a retrotransposon upstream of the *Avr* gene *PWT3* caused the wheat blast isolate Br116.5 to gain virulence on *Rwt3*-containing cultivars. The observation that four out of six 3BC mutants are virulent because of TE insertions near $AvrPm3^{b2/c2}$ is intriguing and further highlights the relevance of TEs in pathogen evolution. What we

observe after UV light irradiation might mimic (likely with an increased frequency) what also happens in natural settings, where TE induction often occurs because of environmental stress and contributes to evolution (Biémont and Vieira 2006). Our results emphasize the importance of considering also TE transpositions as phenotype-causing mutations in mutagenesis screenings. Despite the advantages mentioned, AvrXpose also has some limitations. First, it relies on the quality of TE annotation and consensus sequences (Stritt and Roulin 2021). In the case of *Bgt*, it performed well, because TEs are well characterized (Parlange et al. 2011; Wicker et al. 2013). However, this may limit this type of analysis in other organisms with poorer TE annotations or for undescribed TEs. For instance, in the case of mutant 3BC_6, the family of the TE inserted close to *AvrPm3*$^{b2/c2}$ was not known, and only the fact that we already knew the *Avr* locus allowed us to find the mutation (Table 2). Ideally, this issue could be circumvented by conducting a global analysis to identify the differentially expressed gene(s) in a specific mutant. Second, our mutant screen is far from saturation, potentially limiting our ability to detect additional genetic components controlling avirulence. For example, we did not find commonly mutated genes in at least two of the 3F+A mutants, despite using different approaches. Regarding mutant 3F+A_4, it remains unclear whether the SNP 2.7 kb upstream of *Bgt-646* is responsible for its phenotype, as it does not have an impact on *Bgt-646* expression at 48 h after infection. The mutation may not correlate with the virulence phenotype, for which the actual cause might be analogous to that of mutants 3F+A_5 and 3F+A_6. In any case, our results suggest that there may be more than one powdery mildew gene affecting specific avirulence, and the lack of saturation in our mutagenesis did not allow us to mutate all of them. Nonetheless, generating a larger number of *Bgt* gain-of-virulence mutants or, eventually, performing more rounds of UV mutagenesis to generate more mutations (as done by Barsoum et al. 2020) could potentially overcome this limitation and allow multiple genetic components governing avirulence to be found.

The genetic complexity of avirulence differs for highly similar alleles of the *Pm3* immune receptor

AvrXpose was immediately able to (re)identify *AvrPm3*$^{b2/c2}$ as the Avr recognized by the Pm3b and Pm3c pair. Interestingly, this was not the case for *Pm3a* and *Pm3f*, although it was found that, as for the *Pm3b* and *Pm3c* case, *Pm3a* has overlapping but broader resistance than *Pm3f*. Indeed, the 3F mutants were not virulent on *Pm3a*. Interestingly, we never identified a gain-of-virulence mutant on *Pm3d* or *Pm3e* despite both belonging to the same *Pm3* allelic series. Bourras et al. (2015) suggested that, as for *Pm3a*, avirulence on *Pm3d* is determined by three distinct genetic components in the pathogen, among which the suppressor *SvrPm3* and the canonical effector *AvrPm3d* have been identified (Bourras et al. 2019). The fact that we did not find *Pm3d*-virulent mutants supports the hypothesis that Pm3d can recognize two Avrs, similar to what was observed for Pm1a (Kloppe et al. 2023). The case of *Pm3e* may also be similar to that of *Pm3d*, as *Pm3e* differs by only three point mutations from *Pm3d* (Yahiaoui et al. 2006). Identifying avirulence components could be further complicated if they are multicopy genes. This may be the case for *AvrPm3*^{a3} as well.

We conclude that the *Pm3-AvrPm3* system is much more complex than a single gene-for-gene interaction, and further investigation is needed to unravel all the components involved from the pathogen side. Nevertheless, AvrXpose expands our knowledge of the *Pm3-AvrPm3* system by unraveling the genetics behind *Pm3* allelic specificity and recognition of different *Avr* components by clarifying the effect of specific mutations in some *Avrs* on *Pm3* race-specific avirulence.

Bgt-646 is a novel, specific regulator of avirulence

Three independent mutants carrying mutations in *Bgt-646* were virulent on both *Pm3a* and *WTK4*. We confirmed the specificity of that gain of virulence by phenotyping several *Pm* gene-containing lines, which remained resistant, confirming that *Bgt-646* plays a role in regulating avirulence specifically on *Pm3a* and *WTK4*. Notably, avirulence to *Pm24*, a tandem ki-

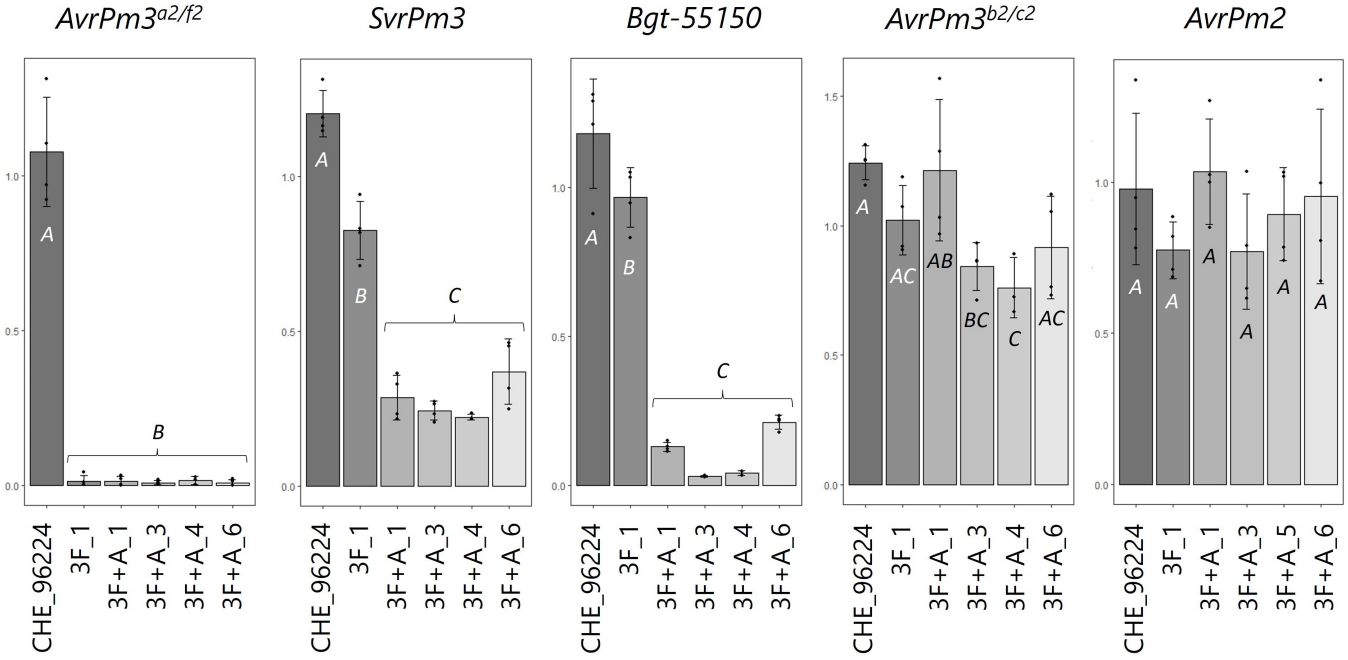

Fig. 6. The 3F+A mutants have a reduced expression of specific *Blumeria graminis* f. sp. *tritici* (*Bgt*) effector genes. As a control, we tested *AvrPm3*$^{a2/f2}$ expression, which is absent in the parental isolate, 3F_1, because of a large deletion and, consequently, in all 3F+A mutants. The expression normalized to the reference gene *GAPDH* is depicted on the *y* axis. Four biological replicates were tested. Significance and *P* values were calculated with a two-sided analysis of variance (ANOVA) followed by a Tukey's HSD test (Supplementary Table S11). A significance threshold of $P < 0.05$ was chosen; bars with the same letter are not significantly different.

nase *R* gene like *WTK4* (Lu et al. 2020), was also not affected in these mutants. It seems unlikely that *Bgt-646* encodes for the effector recognized by Pm3a or WTK4 because of its large size, the absence of a RNAse-like fold structure, and the lack of a predicted signal peptide. The putative DNA-binding capacity, the predicted nuclear localization, and the expression downregulation of specific *Bgt* effectors led us to hypothesize that *Bgt-646* controls race-specific avirulence in *Bgt* by influencing putative *Avr* gene expression (Fig. 7). Experimental evidence showing subcellular localization and DNA-binding capacity of Bgt-646 could further clarify its role in expression regulation. Additional 3F+A mutants with intact *Bgt-646* indicate that, in addition to *Bgt-646*, there are one or more additional components (shown as CoF6 in Fig. 7) controlling avirulence specifically on both the *Pm3a* and *WTK4 R* genes. Interestingly, regardless of the presence of an intact *Bgt-646*, all 3F+A mutants tested showed the same effector downregulation pattern, yet another indication that both *Bgt-646* and the unidentified component(s) (e.g., *CoF6*) contribute to the same regulatory mechanism, which argues against the unidentified component(s) being the recognized effector(s). Moreover, if *Bgt-646* and the unidentified component had the same function, we would not observe virulence when only one was mutated because of redundancy. Therefore, they may be part of a higher-order regulatory complex, and both are required to regulate the expression of specific effectors. If either of them was mutated, the result would be a loss of avirulence (Fig. 7).

However, the mechanisms by which *Bgt-646* affects expression remain unclear. It has been previously described that knockout of a regulatory gene can affect the expression of effector genes. For example, *Sge1* is a known transcriptional regulator that specifically downregulates effector expression in different pathogenic fungi (Michielse et al. 2009; Santhanam and Thomma 2013). On the other hand, ankyrin repeat-containing proteins playing a role in pathogenesis have been described, such as RARP-1, a periplasmic protein that supports infection of

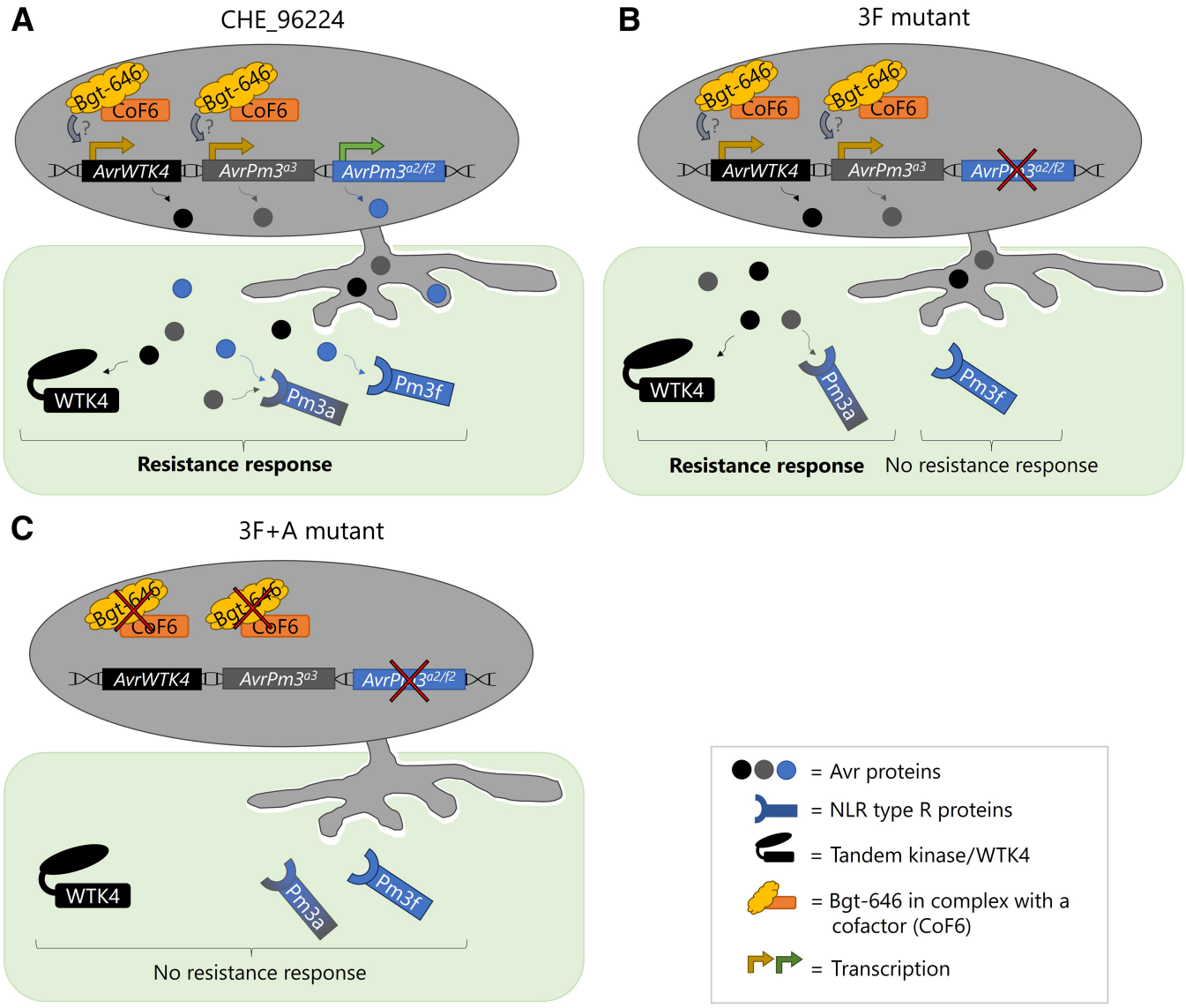

Fig. 7. Model of the regulation of *Avr* expression in the different mutants. **A,** An avirulent *Blumeria graminis* f. sp. *tritici* (*Bgt*) isolate (in grey) infecting a host cell (in green). Bgt-646 (in yellow), together with a cofactor, here named CoF6 (in orange), activates the transcription of different effectors, among them the yet unknown *AvrWTK4* and *AvrPm3*^{a3}, which are secreted and recognized by hosts having the corresponding R proteins, WTK4, Pm3f, or Pm3a, respectively. **B,** A 3F mutant lacking *AvrPm3*$^{a2/f2}$, hence not detected by *Pm3f*-containing hosts, is represented. Because it still expresses *AvrPm3*^{a3}, it will activate the immune response in *Pm3a*-containing hosts. **C,** A 3F+A mutant lacking *AvrPm3*$^{a2/f2}$, as well as *Bgt-646* or *CoF6*, will not express and secrete AvrWTK4 and AvrPm3^{a3}, making it unrecognizable by *Pm3f*-, *Pm3a*-, or *WTK4*-containing hosts. NLR, nucleotide-binding leucine-rich repeat.

the bacterial pathogen *Rickettsia parkeri* (Sanderlin et al. 2022). Ankyrin repeat proteins have often been shown to have transcriptional functions, at least in plants (Vo et al. 2015). In fungi, one well-studied group of proteins with transcriptional regulatory functions, the APSES family proteins, have DNA-binding domains and additional domains, often ankyrin repeats (Zhao et al. 2015). Although *Bgt-646* does not have the conserved DNA-binding domain of the APSES family, the prediction of DNA-binding sites in *Bgt-646* may indicate a similar expression-controlling function.

A chromosome-scale assembly of the 3F+A mutants could reveal whether there are additional mutated genes that we have not found with AvrXpose. Furthermore, a transcriptomic experiment comparing gene expression of the 3F+A mutants with their avirulent parent would unravel the complete set of differentially regulated effectors, and thus also support the identification of the still unknown *AvrPm3*^{a3} and *AvrWTK4*.

This study aimed to develop a method for finding *Avr*s and unraveling additional genetic components involved in avirulence on different *Pm3* alleles. We demonstrated the potential of AvrXpose to discover *Avr* effectors, as well as a conserved regulatory factor (i.e., *Bgt-646*) and showed that this methodology also allows us to unravel the different mechanisms of recognition evasion in different *Avr-R* systems.

Materials and Methods

Plant and fungal material

Wheat cultivars Kanzler (accession number K-57220) and Chancellor (accession number K-51404) were used as mildew-susceptible controls and to maintain the powdery mildew isolates. NILs Asosan/8*Chancellor, Chul/8*Chancellor, Sonora/8*Chancellor, Kolibri, W150, and Michigan Amber/8*Chancellor (described by Brunner et al. 2010) were used to test for *Pm3a*-, *Pm3b*-, *Pm3c*-, *Pm3d*-, *Pm3e*-, and *Pm3f*-mediated resistance, respectively. The transgenic line E#2 was used to assess *Pm3e*-mediated resistance (Koller et al. 2019). To test the virulence specificity of the mutant wheat mildew isolates, we used the wheat NILs Axminster/8*Chancellor, containing *Pm1a* (described by Hewitt et al. 2021); Federation*4/Ulka, containing *Pm2* (Sánchez-Martín et al. 2016); Khapli/8*Chancellor//8*Federation, containing *Pm4a*; Federation*8/W804, containing *Pm4b* (described by Sánchez-Martín et al. 2021); Kavkaz/4*Federation, containing *Pm8* (Hurni et al. 2013); and USDA_Pm24, containing *Pm24*, and the 1AL.1RS translocation line Amigo, containing *Pm17* (described by Müller et al. 2022). *A. tauschii* accessions from a diversity panel (e.g., TOWWC063, TOWWC087, TOWWC112, and TOWWC154; Arora et al. 2019) containing the resistance gene *WTK4* were used to assess powdery mildew virulence on *WTK4*.

Bgt isolate CHE_96224 (Müller et al. 2019) and the derived *Bgt* mutants were used for phenotyping experiments to evaluate gain-of-virulence phenotypes. CHE_96224 is avirulent (no visible disease symptoms observed) on all previously mentioned *R* gene-containing wheat and *A. tauschii* lines, except for the *Pm1a*- and *Pm8*-containing lines, while all the *Bgt* mutants show virulence on one or more of the previously described wheat lines.

Mutagenesis and phenotyping experiments

Plants used for mutagenesis and phenotyping experiments were grown (16-h light, 8-h dark, 18°C, and 60% humidity) for 9 to 12 days in the case of wheat and 12 to 17 days for *A. tauschii* lines. Leaves were then cut into 3-cm fragments and placed in Petri dishes containing water agar supplemented with benzimidazole (5 ppm, MERCK, 51-17-2). They were then spray-inoculated with *Bgt* isolates, as described by Hurni et al. (2013). At least three biological replicates were used per inoculation.

For mutagenesis, *Bgt* isolates CHE_96224 or 3F_1 were grown on the susceptible wheat cultivar Kanzler for 7 days, irradiated with UV-C light in a UV cabinet (Herolab Crosslinker CL-1, 254-nm version) as described by Barsoum et al. (2020), and directly used for inoculation of 9- to 12-day-old Kanzler leaf segments placed on Petri dishes as described earlier (Fig. 1). The irradiation time varied between 2 and 10 min and was adjusted to the time at which 50% leaf coverage by powdery mildew was achieved (usually between 4 and 6 min). For example, if survival was too low after the first irradiation step (e.g., <20% coverage), we irradiated for 2 min in the second step. Conversely, if survival was too high (>80% leaf coverage), we increased the irradiation time to 10 min in the second step. This procedure was repeated twice, resulting in three total rounds of UV irradiation. Finally, the irradiated spore mixture was used to inoculate wheat or *A. tauschii* lines containing different *R* genes. *Bgt* colonies growing on the resistant lines were propagated on freshly cut Kanzler leaves placed on agar Petri dishes. After 4 days, leaf segments containing single colonies were cut and transferred to a new Petri dish. This isolation procedure was repeated twice to ensure genetic homogeneity of the isolated *Bgt* mutants. After sufficient spores were obtained, the phenotypes of the selected mutants were evaluated on a diverse panel of wheat and *A. tauschii* lines containing different *Pm* genes to confirm their virulence spectrum, and spores were collected for DNA extraction and subsequent sequencing. Disease levels were assessed by eye 7 to 8 days after inoculation, and virulence was based on the percentage of the leaf area covered by the fungal mycelia (avirulent: <25%; virulent: >25% leaf coverage).

DNA extraction and whole-genome sequencing

DNA extraction using a chloroform and CTAB-based protocol was performed as described by Bourras et al. (2015). Library preparation and Illumina whole-genome sequencing were performed at the Functional Genomics Center (Zurich, Switzerland) and Novogene (Cambridge, U.K.) using the NovaSeq 6000 technology. Paired-end sequence reads of 150 bp and an insert size of approximately 350 bp generated 1.5 to 13 Gb of sequence data per *Bgt* isolate, resulting in an average genome coverage of 25× to 150×. The other *Bgt* isolates described in this study were previously sequenced using the same technology and DNA extraction protocol. Sequences of CHE_96224 and the isolates used to examine *Bgt-646* haplotype diversity (Supplementary Table S5) are available at NCBI (McNally et al. 2018; Sotiropoulos et al. 2022).

Trimming, mapping, variant calling, and TE detection

To prepare the Illumina reads for subsequent analysis, we trimmed and mapped the reads as described in Sotiropoulos et al. (2022). Briefly, the obtained raw reads were first trimmed for contamination from the Illumina oligo adapter, and the sequence quality was checked using Trimmomatic v. 0.39 (Bolger et al. 2014). The trimmed reads were then mapped to the reference genome of the *Bgt* isolate CHE_96224, v. 3.16 (Müller et al. 2019) using bwa mem v. 0.7 (Li and Durbin 2009). Finally, Samtools v. 1.9 (Li et al. 2009) was used to sort and remove duplicates to subsequently generate and index the mapping (BAM) files used for haplotype calling. Mapping quality and coverage were visually inspected using the integrative genomics viewer IGV (Robinson et al. 2011).

Haplotype calling was performed with Freebayes (Garrison and Marth 2012), applying the parameters -p 1 -m 30 -q 20 -z 0.03 -F 0.7 -3 200, as described in Müller et al. (2019). SNPs and indels were then filtered using Vcftools to obtain variants with less than 10% missing data (Danecek et al. 2011).

The resulting vcf file was transformed into hapmap format using Tassel5 (Bradbury et al. 2007). TE insertions were detected using the software Detettore, with default parameters (Stritt and Roulin 2021). Coverage analysis to detect possibly deleted or duplicated genes was performed using an in-house Python script (retrievable from https://gist.github.com/caldetas/24576da33d1ff91057ecabb1c5a3b6af). The annotation version 4.20 of CHE_96224 was used to select variants less than 1.5 or 2 kb away (for SNPs and TE insertions, respectively) from annotated genes. To avoid overlooking variants, we also checked whether we found variants in one mutant close to variants in other mutants. Only variants uniquely occurring in a mutant were retained for further analyses (Supplementary Tables S1 to S3). All variants close to annotated genes were then visually inspected and confirmed using IGV.

Bgt-646 domains and motifs predictions

A variety of software programs were used to predict the protein domains and properties of *Bgt-646*. DNABIND, DP-bind, and DRNApred were used to predict DNA binding residues (Hwang et al. 2007; Szilágyi and Skolnick 2006; Yan and Kurgan 2017). ScanPROSITE, LOCALIZER, and WoLF PSORT were used to predict domains and subcellular localization (https://prosite.expasy.org; Horton et al. 2007; Sperschneider et al. 2017). Details and prediction results are described in Supplementary Tables S6 to S10.

Multiple sequence alignment and phylogenetic tree of *Bgt-646* homologs

Homologs of Bgt-646 were searched in the NCBI database using Protein Blast with default parameters (https://blast.ncbi.nlm.nih.gov). A multiple sequence alignment was performed using COBALT (Papadopoulos and Agarwala 2007), available directly from the NCBI website. COBALT uses information from conserved domain and protein motif databases and sequence similarity based on RPS-BLAST, BLASTP, and PHI-BLAST. The multiple alignment is shown in Supplementary Figure S7. A phylogenetic tree was constructed using FastTree (Price et al. 2009), visualized and modified using FigTree v. 1.4.4 (retrievable from https://github.com/rambaut/figtree/releases/tag/v1.4.4). The Phyre2 web portal was used to predict structural homologs (Kelley et al. 2015).

PCR, qPCR experiments, and statistical analyses

PCRs for amplification of TE insertions were performed using Phusion High-Fidelity DNA Polymerase (M0530S, New England BioLabs) according to the manufacturer's recommendations, with an annealing temperature of 59°C and an extension time of 3 min.

To study the expression of specific genes, RT-qPCR experiments were performed according to the MIQE guidelines (Bustin et al. 2009). mRNA samples were extracted from infected leaf material obtained from three to five independent biological replicates 2 days after *Bgt* infection, using the Dynabeads mRNA DIRECT Kit (Invitrogen). cDNA was then synthesized using the Maxima H Minus First Strand cDNA Synthesis Kit (ThermoFisher), according to the manufacturer's instructions. Fungal glyceraldehyde 3-phosphate dehydrogenase ($GAPDH_{Bgt}$) was used as an internal control to normalize gene expression. The KAPA SYBR FAST qPCR kit (Kapa Biosystems) was used to amplify the gene of interest and the internal control in a CFX384 Touch Real-Time PCR Detection System (Bio-Rad). Gene expression was analyzed with the CFX Maestro software v. 3.1 (Bio-Rad). To assess statistical differences between groups, an analysis of variance (ANOVA) was performed, followed by a Tukey's HSD (honestly significant difference) test. The analyses were performed in R using the functions *aov* and *TukeyHSD*, respectively. Letters corresponding to significance groups have been assigned using *glht* and *cld* functions of the multcomp package (Bretz et al. 2010). The results of the statistical analyses are described in Supplementary Table S11.

PCR and RT-qPCR primers for promoter regions, reference, and target genes of *Bgt* are listed in Supplementary Table S12.

Data Availability

Raw FASTA sequences of all *Bgt* mutants generated in this study are available through NCBI (BioProject ID: PRJNA1016363).

Acknowledgments

We thank Gerhard Herren and Victoria Widrig for the help with RT-qPCR and for technical support, Lukas Kunz and Marion C. Müller for fruitful discussions and material, and the Functional Genomics Center Zurich of the University of Zurich (FCGZ) for sequencing. We also thank Christina Cowger, Small Grains Pathologist, USDA-ARS, Department of Plant Pathology, North Carolina State University, for providing us with the *Pm24* differential line.

Literature Cited

Arora, S., Steuernagel, B., Gaurav, K., Chandramohan, S., Long, Y., Matny, O., Johnson, R., Enk, J., Periyannan, S., Singh, N., Asyraf Md Hatta, M., Athiyannan, N., Cheema, J., Yu, G., Kangara, N., Ghosh, S., Szabo, L. J., Poland, J., Bariana, H., Jones, J. D. G., Bentley, A. R., Ayliffe, M., Olson, E., Xu, S. S., Steffenson, B. J., Lagudah, E., and Wulff, B. B. H. 2019. Resistance gene cloning from a wild crop relative by sequence capture and association genetics. Nat. Biotechnol. 37:139-143.

Barsoum, M., Kusch, S., Frantzeskakis, L., Schaffrath, U., and Panstruga, R. 2020. Ultraviolet mutagenesis coupled with next-generation sequencing as a method for functional interrogation of powdery mildew genomes. Mol. Plant-Microbe Interact. 33:1008-1021.

Biémont, C., and Vieira, C. 2006. Junk DNA as an evolutionary force. Nature 443:521-524.

Bolger, A. M., Lohse, M., and Usadel, B. 2014. Trimmomatic: A flexible trimmer for Illumina sequence data. Bioinformatics 30:2114-2120.

Bourras, S., Kunz, L., Xue, M., Praz, C. R., Müller, M. C., Kälin, C., Schläfli, M., Ackermann, P., Flückiger, S., Parlange, F., Menardo, F., Schaefer, L. K., Ben-David, R., Roffler, S., Oberhaensli, S., Widrig, V., Lindner, S., Isaksson, J., Wicker, T., Yu, D., and Keller, B. 2019. The *AvrPm3-Pm3* effector-NLR interactions control both race-specific resistance and host-specificity of cereal mildews on wheat. Nat. Commun. 10:2292.

Bourras, S., McNally, K. E., Ben-David, R., Parlange, F., Roffler, S., Praz, C. R., Oberhaensli, S., Menardo, F., Stirnweis, D., Frenkel, Z., Schaefer, L. K., Flückiger, S., Treier, G., Herren, G., Korol, A. B., Wicker, T., and Keller, B. 2015. Multiple avirulence loci and allele-specific effector recognition control the *Pm3* race-specific resistance of wheat to powdery mildew. Plant Cell 27:2991-3012.

Bourras, S., McNally, K. E., Müller, M. C., Wicker, T., and Keller, B. 2016. Avirulence genes in cereal powdery mildews: The gene-for-gene hypothesis 2.0. Front. Plant Sci. 7:241.

Bradbury, P. J., Zhang, Z., Kroon, D. E., Casstevens, T. M., Ramdoss, Y., and Buckler, E. S. 2007. TASSEL: Software for association mapping of complex traits in diverse samples. Bioinformatics 23:2633-2635.

Bretz, F., Hothorn, T., and Westfall, P. 2010. Multiple Comparisons Using R. 1st ed. Chapman and Hall/CRC, New York.

Brueggeman, R., Rostoks, N., Kudrna, D., Kilian, A., Han, F., Chen, J., Druka, A., Steffenson, B., and Kleinhofs, A. 2002. The barley stem rust-resistance gene *Rpg1* is a novel disease-resistance gene with homology to receptor kinases. Proc. Natl. Acad. Sci. U.S.A. 99:9328-9333.

Brunner, S., Hurni, S., Streckeisen, P., Mayr, G., Albrecht, M., Yahiaoui, N., and Keller, B. 2010. Intragenic allele pyramiding combines different specificities of wheat *Pm3* resistance alleles. Plant J. 64:433-445.

Bustin, S. A., Benes, V., Garson, J. A., Hellemans, J., Huggett, J., Kubista, M., Mueller, R., Nolan, T., Pfaffl, M. W., Shipley, G. L., Vandesompele, J., and Wittwer, C. T. 2009. The MIQE Guidelines: Minimum information for publication of quantitative real-time PCR experiments. Clin. Chem. 55:611-622.

Cao, Y., Kümmel, F., Logemann, E., Gebauer, J. M., Lawson, A. W., Yu, D., Uthoff, M., Keller, B., Jirschitzka, J., Baumann, U., Tsuda, K., Chai, J., and Schulze-Lefert, P. 2023. Structural polymorphisms within a common

powdery mildew effector scaffold as a driver of coevolution with cereal immune receptors. Proc. Natl. Acad. Sci. U.S.A. 120:e2307604120.

Chen, J., Upadhyaya, N. M., Ortiz, D., Sperschneider, J., Li, F., Bouton, C., Breen, S., Dong, C., Xu, B., Zhang, X., Mago, R., Newell, K., Xia, X., Bernoux, M., Taylor, J. M., Steffenson, B., Jin, Y., Zhang, P., Kanyuka, K., Figueroa, M., Ellis, J. G., Park, R. F., and Dodds, P. N. 2017. Loss of *AvrSr50* by somatic exchange in stem rust leads to virulence for *Sr50* resistance in wheat. Science 358:1607-1610.

Danecek, P., Auton, A., Abecasis, G., Albers, C. A., Banks, E., DePristo, M. A., Handsaker, R. E., Lunter, G., Marth, G. T., Sherry, S. T., McVean, G., Durbin, R., and 1000 Genomes Project Analysis Group. 2011. The variant call format and VCFtools. Bioinformatics 27:2156-2158.

Dodds, P. N., and Rathjen, J. P. 2010. Plant immunity: Towards an integrated view of plant-pathogen interactions. Nat. Rev. Genet. 11:539-548.

Faino, L., Seidl, M. F., Shi-Kunne, X., Pauper, M., van den Berg, G. C. M., Wittenberg, A. H. J., and Thomma, B. P. H. J. 2016. Transposons passively and actively contribute to evolution of the two-speed genome of a fungal pathogen. Genome Res. 26:1091-1100.

Frantzeskakis, L., Kracher, B., Kusch, S., Yoshikawa-Maekawa, M., Bauer, S., Pedersen, C., Spanu, P. D., Maekawa, T., Schulze-Lefert, P., and Panstruga, R. 2018. Signatures of host specialization and a recent transposable element burst in the dynamic one-speed genome of the fungal barley powdery mildew pathogen. BMC Genomics 19:381.

Garrison, E., and Marth, G. 2012. Haplotype-based variant detection from short-read sequencing. arXiv 1207.3907. http://arxiv.org/abs/1207.3907

Gaurav, K., Arora, S., Silva, P., Sánchez-Martín, J., Horsnell, R., Gao, L., Brar, G. S., Widrig, V., John Raupp, W., Singh, N., Wu, S., Kale, S. M., Chinoy, C., Nicholson, P., Quiroz-Chávez, J., Simmonds, J., Hayta, S., Smedley, M. A., Harwood, W., Pearce, S., Gilbert, D., Kangara, N., Gardener, C., Forner-Martínez, M., Liu, J., Yu, G., Boden, S. A., Pascucci, A., Ghosh, S., Hafeez, A. N., O'Hara, T., Waites, J., Cheema, J., Steuernagel, B., Patpour, M., Justesen, A. F., Liu, S., Rudd, J. C., Avni, R., Sharon, A., Steiner, B., Kirana, R. P., Buerstmayr, H., Mehrabi, A. A., Nasyrova, F. Y., Chayut, N., Matny, O., Steffenson, B. J., Sandhu, N., Chhuneja, P., Lagudah, E., Elkot, A. F., Tyrrell, S., Bian, X., Davey, R. P., Simonsen, M., Schauser, L., Tiwari, V. K., Randy Kutcher, H., Hucl, P., Li, A., Liu, D.-C., Mao, L., Xu, S., Brown-Guedira, G., Faris, J., Dvorak, J., Luo, M.-C., Krasileva, K., Lux, T., Artmeier, S., Mayer, K. F. X., Uauy, C., Mascher, M., Bentley, A. R., Keller, B., Poland, J., and Wulff, B. B. H. 2022. Population genomic analysis of *Aegilops tauschii* identifies targets for bread wheat improvement. Nat. Biotechnol. 40:422-431.

Hewitt, T., Müller, M. C., Molnár, I., Mascher, M., Holušová, K., Šimková, H., Kunz, L., Zhang, J., Li, J., Bhatt, D., Sharma, R., Schudel, S., Yu, G., Steuernagel, B., Periyannan, S., Wulff, B., Ayliffe, M., McIntosh, R., Keller, B., Lagudah, E., and Zhang, P. 2021. A highly differentiated region of wheat chromosome 7AL encodes a *Pm1a* immune receptor that recognizes its corresponding *AvrPm1a* effector from *Blumeria graminis*. New Phytol. 229:2812-2826.

Horton, P., Park, K.-J., Obayashi, T., Fujita, N., Harada, H., Adams-Collier, C. J., and Nakai, K. 2007. WoLF PSORT: Protein localization predictor. Nucleic Acids Res. 35:W585-W587.

Hurni, S., Brunner, S., Buchmann, G., Herren, G., Jordan, T., Krukowski, P., Wicker, T., Yahiaoui, N., Mago, R., and Keller, B. 2013. Rye *Pm8* and wheat *Pm3* are orthologous genes and show evolutionary conservation of resistance function against powdery mildew. Plant J. 76:957-969.

Hwang, S., Gou, Z., and Kuznetsov, I. B. 2007. DP-Bind: A Web server for sequence-based prediction of DNA-binding residues in DNA-binding proteins. Bioinformatics 23:634-636.

Inoue, Y., Vy, T. T. P., Yoshida, K., Asano, H., Mitsuoka, C., Asuke, S., Anh, V. L., Cumagun, C. J. R., Chuma, I., Terauchi, R., Kato, K., Mitchell, T., Valent, B., Farman, M., and Tosa, Y. 2017. Evolution of the wheat blast fungus through functional losses in a host specificity determinant. Science 357:80-83.

Jones, J. D. G., and Dangl, J. L. 2006. The plant immune system. Nature 444:323-329.

Kangara, N., Kurowski, T. J., Radhakrishnan, G. V., Ghosh, S., Cook, N. M., Yu, G., Arora, S., Steffenson, B. J., Figueroa, M., Mohareb, F., Saunders, D. G. O., and Wulff, B. B. H. 2020. Mutagenesis of *Puccinia graminis* f. sp. *tritici* and selection of gain-of-virulence mutants. Front. Plant Sci. 11:570180.

Kelley, L. A., Mezulis, S., Yates, C. M., Wass, M. N., and Sternberg, M. J. E. 2015. The Phyre2 web portal for protein modeling, prediction and analysis. Nat. Protoc. 10:845-858.

Kloppe, T., Whetten, R. B., Kim, S.-B., Powell, O. R., Lück, S., Douchkov, D., Whetten, R. W., Hulse-Kemp, A. M., Balint-Kurti, P., and Cowger, C. 2023. Two pathogen loci determine *Blumeria graminis* f. sp. *tritici* virulence to wheat resistance gene *Pm1a*. New Phytol. 238:1546-1561.

Klymiuk, V., Coaker, G., Fahima, T., and Pozniak, C. J. 2021. Tandem protein kinases emerge as new regulators of plant immunity. Mol. Plant-Microbe Interact. 34:1094-1102.

Koller, T., Brunner, S., Herren, G., Sanchez-Martin, J., Hurni, S., and Keller, B. 2019. Field grown transgenic *Pm3e* wheat lines show powdery mildew resistance and no fitness costs associated with high transgene expression. Transgenic Res. 28:9-20.

Li, H., and Durbin, R. 2009. Fast and accurate short read alignment with Burrows-Wheeler transform. Bioinformatics 25:1754-1760.

Li, H., Handsaker, B., Wysoker, A., Fennell, T., Ruan, J., Homer, N., Marth, G., Abecasis, G., Durbin, R., and 1000 Genome Project Data Processing Subgroup. 2009. The Sequence Alignment/Map format and SAMtools. Bioinformatics 25:2078-2079.

Li, Y., Wang, M., See, D. R., and Chen, X. 2019. Ethyl-methanesulfonate mutagenesis generated diverse isolates of *Puccinia striiformis* f. sp. *tritici*, the wheat stripe rust pathogen. World J. Microbiol. Biotechnol. 35:28.

Lo Presti, L., Lanver, D., Schweizer, G., Tanaka, S., Liang, L., Tollot, M., Zuccaro, A., Reissmann, S., and Kahmann, R. 2015. Fungal effectors and plant susceptibility. Annu. Rev. Plant Biol. 66:513-545.

Lu, P., Guo, L., Wang, Z., Li, B., Li, J., Li, Y., Qiu, D., Shi, W., Yang, L., Wang, N., Guo, G., Xie, J., Wu, Q., Chen, Y., Li, M., Zhang, H., Dong, L., Zhang, P., Zhu, K., Yu, D., Zhang, Y., Deal, K. R., Huo, N., Liu, C., Luo, M.-C., Dvorak, J., Gu, Y. Q., Li, H., and Liu, Z. 2020. A rare gain of function mutation in a wheat tandem kinase confers resistance to powdery mildew. Nat. Commun. 11:680.

Lu, X., Kracher, B., Saur, I. M. L., Bauer, S., Ellwood, S. R., Wise, R., Yaeno, T., Maekawa, T., and Schulze-Lefert, P. 2016. Allelic barley MLA immune receptors recognize sequence-unrelated avirulence effectors of the powdery mildew pathogen. Proc. Natl. Acad. Sci. U.S.A. 113:E6486-E6495.

McNally, K. E., Menardo, F., Lüthi, L., Praz, C. R., Müller, M. C., Kunz, L., Ben-David, R., Chandrasekhar, K., Dinoor, A., Cowger, C., Meyers, E., Xue, M., Zeng, F., Gong, S., Yu, D., Bourras, S., and Keller, B. 2018. Distinct domains of the AVRPM3$^{A2/F2}$ avirulence protein from wheat powdery mildew are involved in immune receptor recognition and putative effector function. New Phytol. 218:681-695.

Michielse, C. B., van Wijk, R., Reijnen, L., Manders, E. M. M., Boas, S., Olivain, C., Alabouvette, C., and Rep, M. 2009. The nuclear protein Sge1 of *Fusarium oxysporum* is required for parasitic growth. PLoS Pathog. 5:e1000637.

Müller, M. C., Kunz, L., Schudel, S., Lawson, A. W., Kammerecker, S., Isaksson, J., Wyler, M., Graf, J., Sotiropoulos, A. G., Praz, C. R., Manser, B., Wicker, T., Bourras, S., and Keller, B. 2022. Ancient variation of the *AvrPm17* gene in powdery mildew limits the effectiveness of the introgressed rye *Pm17* resistance gene in wheat. Proc. Natl. Acad. Sci. U.S.A. 119:e2108808119.

Müller, M. C., Praz, C. R., Sotiropoulos, A. G., Menardo, F., Kunz, L., Schudel, S., Oberhänsli, S., Poretti, M., Wehrli, A., Bourras, S., Keller, B., and Wicker, T. 2019. A chromosome-scale genome assembly reveals a highly dynamic effector repertoire of wheat powdery mildew. New Phytol. 221:2176-2189.

Nirmala, J., Drader, T., Lawrence, P. K., Yin, C., Hulbert, S., Steber, C. M., Steffenson, B. J., Szabo, L. J., von Wettstein, D., and Kleinhofs, A. 2011. Concerted action of two avirulent spore effectors activates *Reaction to Puccinia graminis 1* (*Rpg1*)-mediated cereal stem rust resistance. Proc. Natl. Acad. Sci. U.S.A. 108:14676-14681.

Papadopoulos, J. S., and Agarwala, R. 2007. COBALT: Constraint-based alignment tool for multiple protein sequences. Bioinformatics 23:1073-1079.

Parlange, F., Oberhaensli, S., Breen, J., Platzer, M., Taudien, S., Šimková, H., Wicker, T., Doležel, J., and Keller, B. 2011. A major invasion of transposable elements accounts for the large size of the *Blumeria graminis* f. sp. *tritici* genome. Funct. Integr. Genomics 11:671-677.

Parlange, F., Roffler, S., Menardo, F., Ben-David, R., Bourras, S., McNally, K. E., Oberhaensli, S., Stirnweis, D., Buchmann, G., Wicker, T., and Keller, B. 2015. Genetic and molecular characterization of a locus involved in avirulence of *Blumeria graminis* f. sp. *tritici* on wheat *Pm3* resistance alleles. Fungal Genet. Biol. 82:181-192.

Praz, C. R., Bourras, S., Zeng, F., Sánchez-Martín, J., Menardo, F., Xue, M., Yang, L., Roffler, S., Böni, R., Herren, G., McNally, K. E., Ben-David, R., Parlange, F., Oberhaensli, S., Flückiger, S., Schäfer, L. K., Wicker, T., Yu, D., and Keller, B. 2017. *AvrPm2* encodes an RNase-like avirulence effector which is conserved in the two different specialized forms of wheat and rye powdery mildew fungus. New Phytol. 213:1301-1314.

Price, M. N., Dehal, P. S., and Arkin, A. P. 2009. FastTree: Computing large minimum evolution trees with profiles instead of a distance matrix. Mol. Biol. Evol. 26:1641-1650.

Robinson, J. T., Thorvaldsdóttir, H., Winckler, W., Guttman, M., Lander, E. S., Getz, G., and Mesirov, J. P. 2011. Integrative genomics viewer. Nat. Biotechnol. 29:24-26.

Salcedo, A., Rutter, W., Wang, S., Akhunova, A., Bolus, S., Chao, S., Anderson, N., De Soto, M. F., Rouse, M., Szabo, L., Bowden, R. L., Dubcovsky, J., and Akhunov, E. 2017. Variation in the *AvrSr35* gene determines *Sr35* resistance against wheat stem rust race Ug99. Science 358:1604-1606.

Sánchez-Martín, J., Bourras, S., and Keller, B. 2018. Diseases affecting wheat and barley: Powdery mildew. Pages 69-93 in: Integrated Disease Management of Wheat and Barley. R. Oliver, ed. Burleigh Dodds, Cambridge, U.K.

Sánchez-Martín, J., and Keller, B. 2021. NLR immune receptors and diverse types of non-NLR proteins control race-specific resistance in *Triticeae*. Curr. Opin. Plant Biol. 62:102053.

Sánchez-Martín, J., Steuernagel, B., Ghosh, S., Herren, G., Hurni, S., Adamski, N., Vrána, J., Kubaláková, M., Krattinger, S. G., Wicker, T., Doležel, J., Keller, B., and Wulff, B. B. H. 2016. Rapid gene isolation in barley and wheat by mutant chromosome sequencing. Genome Biol. 17:221.

Sánchez-Martín, J., Widrig, V., Herren, G., Wicker, T., Zbinden, H., Gronnier, J., Spörri, L., Praz, C. R., Heuberger, M., Kolodziej, M. C., Isaksson, J., Steuernagel, B., Karafiátová, M., Doležel, J., Zipfel, C., and Keller, B. 2021. Wheat *Pm4* resistance to powdery mildew is controlled by alternative splice variants encoding chimeric proteins. Nat. Plants 7: 327-341.

Sánchez-Vallet, A., Fouché, S., Fudal, I., Hartmann, F. E., Soyer, J. L., Tellier, A., and Croll, D. 2018. The genome biology of effector gene evolution in filamentous plant pathogens. Annu. Rev. Phytopathol. 56:21-40.

Sanderlin, A. G., Hanna, R. E., and Lamason, R. L. 2022. The ankyrin repeat protein RARP-1 is a periplasmic factor that supports *Rickettsia parkeri* growth and host cell invasion. J. Bacteriol. 204:e00182-22.

Santhanam, P., and Thomma, B. P. H. J. 2013. *Verticillium dahliae* Sge1 differentially regulates expression of candidate effector genes. Mol. Plant-Microbe Interact. 26:249-256.

Saur, I. M. L., Bauer, S., Kracher, B., Lu, X., Franzeskakis, L., Müller, M. C., Sabelleck, B., Kümmel, F., Panstruga, R., Maekawa, T., and Schulze-Lefert, P. 2019. Multiple pairs of allelic MLA immune receptor-powdery mildew AVR_A effectors argue for a direct recognition mechanism. eLife 8:e44471.

Sherwood, J. E., Slutsky, B., and Somerville, S. C. 1991. Induced morphological and virulence variants of the obligate barley pathogen *Erysiphe graminis* f. sp. *hordei*. Phytopathology 81:1350-1357.

Sotiropoulos, A. G., Arango-Isaza, E., Ban, T., Barbieri, C., Bourras, S., Cowger, C., Czembor, P. C., Ben-David, R., Dinoor, A., Ellwood, S. R., Graf, J., Hatta, K., Helguera, M., Sánchez-Martín, J., McDonald, B. A., Morgounov, A. I., Müller, M. C., Shamanin, V., Shimizu, K. K., Yoshihira, T., Zbinden, H., Keller, B., and Wicker, T. 2022. Global genomic analyses of wheat powdery mildew reveal association of pathogen spread with historical human migration and trade. Nat. Commun. 13:4315.

Sperschneider, J., Catanzariti, A.-M., DeBoer, K., Petre, B., Gardiner, D. M., Singh, K. B., Dodds, P. N., and Taylor, J. M. 2017. LOCALIZER: Subcellular localization prediction of both plant and effector proteins in the plant cell. Sci. Rep. 7:44598.

Stirnweis, D., Milani, S. D., Jordan, T., Keller, B., and Brunner, S. 2014. Substitutions of two amino acids in the nucleotide-binding site domain of a resistance protein enhance the hypersensitive response and enlarge the PM3F resistance spectrum in wheat. Mol. Plant-Microbe Interact. 27:265-276.

Stritt, C., and Roulin, A. C. 2021. Detecting signatures of TE polymorphisms in short-read sequencing data. Pages 177-187 in: Plant Transposable Elements: Methods and Protocols. Methods in Molecular Biology 2250. Springer Nature, New York, NY.

Szilágyi, A., and Skolnick, J. 2006. Efficient prediction of nucleic acid binding function from low-resolution protein structures. J. Mol. Biol. 358: 922-933.

Takamatsu, S. 2004. Phylogeny and evolution of the powdery mildew fungi (Erysiphales, Ascomycota) inferred from nuclear ribosomal DNA sequences. Mycoscience 45:147-157.

Upadhyaya, N. M., Mago, R., Panwar, V., Hewitt, T., Luo, M., Chen, J., Sperschneider, J., Nguyen-Phuc, H., Wang, A., Ortiz, D., Hac, L., Bhatt, D., Li, F., Zhang, J., Ayliffe, M., Figueroa, M., Kanyuka, K., Ellis, J. G., and Dodds, P. N. 2021. Genomics accelerated isolation of a new stem rust avirulence gene–wheat resistance gene pair. Nat. Plants 7: 1220-1228.

Vo, K. T. X., Kim, C.-Y., Chandran, A. K. N., Jung, K.-H., An, G., and Jeon, J.-S. 2015. Molecular insights into the function of ankyrin proteins in plants. J. Plant Biol. 58:271-284.

Wicker, T., Oberhaensli, S., Parlange, F., Buchmann, J. P., Shatalina, M., Roffler, S., Ben-David, R., Doležel, J., Šimková, H., Schulze-Lefert, P., Spanu, P. D., Bruggmann, R., Amselem, J., Quesneville, H., Ver Loren van Themaat, E., Paape, T., Shimizu, K. K., and Keller, B. 2013. The wheat powdery mildew genome shows the unique evolution of an obligate biotroph. Nat. Genet. 45:1092-1096.

Yahiaoui, N., Brunner, S., and Keller, B. 2006. Rapid generation of new powdery mildew resistance genes after wheat domestication. Plant J. 47: 85-98.

Yan, J., and Kurgan, L. 2017. DRNApred, fast sequence-based method that accurately predicts and discriminates DNA- and RNA-binding residues. Nucleic Acids Res. 45:e84.

Zhao, Y., Su, H., Zhou, J., Feng, H., Zhang, K.-Q., and Yang, J. 2015. The APSES family proteins in fungi: Characterizations, evolution and functions. Fungal Genet. Biol. 81:271-280.